Polyhedron 29 (2010) 1784–1795

Contents lists available at ScienceDirect

Polyhedron

journal homepage: www.elsevier.com/locate/poly

Structural characterization of methanol substituted lanthanum halides

Timothy J. Boyle [a,*], Leigh Anna M. Ottley [a], Todd M. Alam [b], Mark A. Rodriguez [c], Pin Yang [d], Sarah K. Mcintyre [b]

[a] Sandia National Laboratories, Advanced Materials Laboratory, 1001 University Boulevard, SE, Albuquerque, NM 87106, USA
[b] Sandia National Laboratories, Department of Electronic and Nanostructured Materials, P.O. Box 5800, Mail Stop 0886, Albuquerque NM 87185-0886, USA
[c] Sandia National Laboratories, Department of Materials Characterization, P.O. Box 5800 Mail Stop 1411, Albuquerque NM 87185-1411, USA
[d] Sandia National Laboratories, Department of Ceramic and Glass, P.O. Box 5800 Mail Stop 0963, Albuquerque NM 87185-0963, USA

ARTICLE INFO

Article history:
Received 24 November 2009
Accepted 17 February 2010
Available online 20 February 2010

Keywords:
Lanthanum
Halides
Scintillators
Methanol
Crystal structure

ABSTRACT

The first study into the alcohol solvation of lanthanum halide [LaX_3] derivatives as a means to lower the processing temperature for the production of the $LaBr_3$ scintillators was undertaken using methanol (MeOH). Initially the de-hydration of $\{[La(\mu\text{-}Br)(H_2O)_7](Br)_2\}_2$ (**1**) was investigated through the simple room temperature dissolution of **1** in MeOH. The mixed solvate monomeric $[La(H_2O)_7(MeOH)_2](Br)_3$ (**2**) compound was isolated where the La metal center retains its original 9-coordination through the binding of two additional MeOH solvents but necessitates the transfer of the innersphere Br to the outersphere. In an attempt to in situ dry the reaction mixture of **1** in MeOH over CaH_2, crystals of $[Ca(MeOH)_6](Br)_2$ (**3**) were isolated. Compound **1** dissolved in MeOH at reflux temperatures led to the isolation of an unusual arrangement identified as the salt derivative $\{[LaBr_{2.75}\cdot 5.25(MeOH)]^{+0.25}[LaBr_{3.25}\cdot 4.75(MeOH)]^{-0.25}\}$ (**4**). The fully substituted species was ultimately isolated through the dissolution of dried $LaBr_3$ in MeOH forming the 8-coordinated $[LaBr_3(MeOH)_5]$ (**5**) complex. It was determined that the concentration of the crystallization solution directed the structure isolated (**4** concentrated; **5** dilute) The other LaX_3 derivatives were isolated as $[(MeOH)_4(Cl)_2La(\mu\text{-}Cl)]_2$ (**6**) and $[La(MeOH)_9](I)_3\cdot MeOH$ (**7**). Beryllium Dome XRD analysis indicated that the bulk material for **5** appear to have multiple solvated species, **6** is consistent with the single crystal, and **7** was too broad to elucidate structural aspects. Multinuclear NMR (^{139}La) indicated that these compounds do not retain their structure in MeOD. TGA/DTA data revealed that the de-solvation temperatures of the MeOH derivatives **4**–**6** were slightly higher in comparison to their hydrated counterparts.

© 2010 Elsevier Ltd. All rights reserved.

1. Introduction

Rare earth halide (LnX_3) scintillators are of interest for the detection of γ-radiation due to the fact that these materials display excellent luminosity and proportionality, have high spectral energy resolution at room temperature, exhibit short decay times, and possess sufficient stopping power [1]. Additionally, the linear energy response that LnX_3 materials display also makes them attractive for a variety of imaging applications, including chemical tomography (CT), positron emission tomography (PET), and single photon emission computed tomography (SPECT) [1–8]. As these materials have been studied in depth, it has been reported that in the presence of trace amounts of oxide LaX_3 readily converts to lanthanum oxy halide, which upon hot-pressing yields an opaque material that detracts from the desired scintillator properties [2,3,5,6,8–12]. Since the standard synthetic route to LnX_3 materials involves the reaction of rare earth oxide with the appropriate ammonium halide, commercially available materials inherently have residual oxide present [2,3,5,6,8–12]. Therefore, simple, high-yield routes to oxide free LnX_3 materials are of interest.

In the early 1950's, reports detailing the syntheses and subsequent calorimetric analyses of $LnCl_3\cdot nH_2O$ crystals isolated from the reaction of Ln^o in 1 N HCl(aq) were reported [13,14]. Since that time, no information pertaining to the single crystal structures of the products generated from this or similar (Eq. (1)) methods have been disseminated [15–19]. Recently, we undertook the synthesis and structural characterization of the products isolated from the dissolution of Ln^o in (conc.)HX (Eq. (1)) and for the first time crystallographically characterized all of the $LnX_3\cdot nH_2O$ (Ln = group 3 and lanthanides; X = Cl, Br, I) products [20]. In agreement with the spurious literature structure reports (typically obtained from the hydration of 'anhydrous LaX_3') [21–36], three structure types were noted for this family of compounds: (i) hydrate dimer $[\{(H_2O)_7Ln(\mu\text{-}X)\}_2](X)_2$, (ii) 2IS/1OS as $[LnX_2(H_2O)_8](X)$ and (iii) 3OS as $[Ln(H_2O)_x](X)_3$ (where IS = inner sphere, OS = outer sphere (see Fig. 1a–c) and Ln = group 3, the lanthanide series cations). Table 1 lists the structures adopted by the $LnX_3\cdot nH_2O$ series, isolated

* Corresponding author. Tel.: +1 505 272 7625; fax: +1 505 272 7336.
E-mail address: tjboyle@Sandia.gov (T.J. Boyle).

0277-5387/$ - see front matter © 2010 Elsevier Ltd. All rights reserved.
doi:10.1016/j.poly.2010.02.027

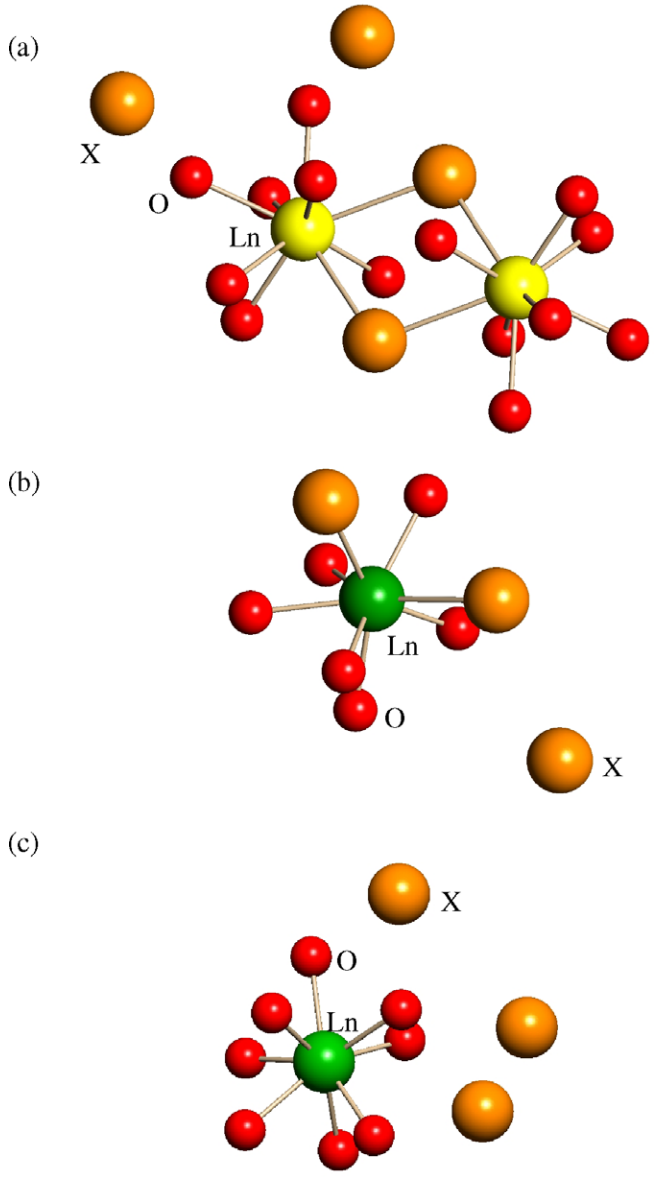

Fig. 1. Schematic structure plots of hydrate species (i) dimer, (ii) 2IS/1OS, and (iii) 3OS. The halides are in orange, the oxides in red, and the lanthanide cations in yellow or green. (For interpretation of the references to colour in this figure legend, the reader is referred to the web version of this article.)

from Eq. (1) [20]. Additional information pertaining to the synthesis and characterization of these compounds is available in the Supplementary data. There are variations in hydration and structural crossover points for these products (Eq. (1)) in comparison to the literature reports [21–36].

$$Ln^{o} + (xs)\ HX \rightarrow Ln(X)_3 \cdot nH_2O \quad (1)$$

$$Ln(X)_3 \cdot nH_2O \xrightarrow[10^{-3}\ Torr]{\Delta} LnX_3 + nH_2O$$

$$Ln = Sc, Y, \text{and the lanthanide series; } X = Cl, Br, I \quad (2)$$

Due to the presence of water, the hydrates are obviously unattractive for scintillator applications; however, in contrast to literature reports [9,10,17,37], it was determined that anhydrous $LaBr_3$ could be isolated by simply heating $[\{(H_2O)_7La(\mu\text{-}Br)\}_2](Br)_2$ (**1**, see Fig. 1a) under vacuum (Eq. (2)) [20]. This gave a simple, reproducible, large-scale route that produced no waste for production of $LaBr_3$ scintillator materials. However, the higher temperatures required for this processing often led to darkening of the material upon hot-pressing into a ceramic disk. This color change was ultimately associated with Br volatility [20]. Therefore, lower processing routes to anhydrous or 'dry' $LaBr_3$ were sought to minimize the Br loss.

Table 1
Structural arrangements recorded for $LnX_3 \cdot nH_2O$ family of compounds isolated from the reaction of Ln^{o} in (conc.) HX [20].

Ln	Chloride				Bromide				Iodide			
	Solv	IS	OS	Nu	Solv	IS	OS	Nu	Solv	IS	OS	Nu
La	7	2(μ)	4	2	7	2(μ)	4	2	9	0	3	1
Ce	7	2(μ)	4	2	7	2(μ)	4	2	9	0	3	1
Pr	7	2(μ)	4	2	7	2(μ)	4	2	9	0	3	1
Nd	6	2	1	1	6	2	1	1	9	0	3	1
Sm	6	2	1	1	6	2	1	1	9	0	3	1
Eu	6	2	1	1	6	2	1	1	9	0	3	1
Gd	6	2	1	1	6	2	1	1	9	0	3	1
Tb	6	2	1	1	6	2	1	1	9	0	3	1
Dy	6	2	1	1	6	2	1	1	9	0	3	1
Ho	6	2	1	1	8	0	3	1	9	0	3	1
Y	6	2	1	1	8	0	3	1	---	---	---	---
Er	6	2	1	1	8	0	3	1	9	0	3	1
Tm	6	2	1	1	8	0	3	1	8	0	3	1
Yb	6	2	1	1	8	0	3	1	8	0	3	1
Lu	6	2	1	1	8	0	3	1	8	0	3	1
Sc	4	2	1	1	7	0	3	1	7	0	3	1

Ln = lanthanide; Solv = number of H_2O bound per metal; IS = inner sphere; OS = outer sphere; Nu = nuclearity; — structure not solved.
Color Key – different shades indicate slightly different structure types: Green = (dimer) $[Ln(\mu\text{-}X)(H_2O)_7]_2(X)_4$; Brown (2IS/1OS) $[LnX_2(H_2O)_6](X)$ or $[ScCl_2(H_2O)_4][Cl \cdot H_2O]$; Blue (3OS) $[Ln(H_2O)_n](X)_3$.

One approach to remedy this problem was to replace the bound waters of **1** with other Lewis bases that were less strongly bound, with a particular emphasis on alcohol (HOR) derivatives [11,18,19,38–73]. The HOR solvents were of interest since it was reasoned they were strong enough to displace the bound water but potentially offered lower de-solvation temperatures. Reports on the structural aspects of Lewis basic functionalized LnX_3 compounds have been extensive [18,19], with a substantial number of compounds possessing the fundamental 'Ln, HOR, 3X' [38–73] composition. However, most of the HOR derivatives were either part of a larger organic moiety or had a large organic ligand bound to the metal. Recently Boatner and co-workers reported on the crystal structure of simple MeOH derivative as $[(MeOH)_4(Cl)_2Ce(\mu\text{-}Cl)]_2$ (MeOH = CH_3OH = methanol), which was also reported to be the first example of a metal–organic scintillator [72,73].

Based on the lack of ROH derivatives of LaX_3 and our interest in dehydrating **1** [20], it became of interest to understand the structural aspects of LaX_3 in MeOH and determine their physical properties. The products isolated through various synthetic attempts included $[La(H_2O)_7(MeOH)_2](Br)_3$ (**2**), $[Ca(MeOH)_6](Br)_2$ (**3**), $\{[LaBr_{2.75} \cdot 5.25(MeOH)]^{+0.25}[LaBr_{3.25} \cdot 4.75(MeOH)]^{-0.25}\}$ (**4**) and the methanolation of LnX_3 to yield $[LaBr_3(MeOH)_5]$ (**5**) $[(MeOH)_4(Cl)_2La(\mu\text{-}Cl)]_2$ (**6**) and $[La(MeOH)_9](I)_3 \cdot MeOH$ (**7**). The synthesis and characterization of these compounds and their dehydration are presented below.

2. Experimental

All compounds described below were handled with rigorous exclusion of air and water using standard Schlenk line and glove box techniques unless otherwise noted. Analytical data were collected on dried crystalline samples. All solvents were used as received (from Aldrich and Alfa Aesar) without further purification, including: MeOH (anhydrous, Sure/Seal™ bottle), conc. HCl (aq, 37%), conc. HBr (aq, 48%), conc. HI (aq, 55%), CaH_2, and La^{o}.

Compound **1** (Fig. 1a) and LaX_3 where X = Br, Cl and I were synthesized according to Eqs. (1) and (2) [20]. Yields approached quantitative for each reaction investigated.

2.1. $[La(H_2O)_7(MeOH)_2](Br)_3$ (**2**)

On the bench-top, a sample of **1** (1.00 g, 1.02 mmol) in a vial was dissolved in MeOH (20 mL) and stirred for 2–3 h. After this time, the reaction was removed from the stir plate and set aside with the cap loose to allow any volatile material to slowly evaporate, until the X-ray quality crystals of **2** were isolated. ^{139}La (56.5 MHz, MeOD) $\delta = -32.7$ ppm.

2.2. $[Ca(MeOH)_6](Br)_2$ (**3**)

CaH_2 (0.100 g) was added to mixture of $LaBr_3$ (1.00 g, 2.64 mmol) in MeOH (25 mL) and allowed to stir. The CaH_2 dissolved to generate a clear solution. Upon slow evaporation, crystals of **3** were isolated.

2.3. $\{[LaBr_{2.75}\cdot 5.25(MeOH)]^{+0.25}[LaBr_{3.25}\cdot 4.75(MeOH)]^{-0.25}\}$ (**4**)

On a Schlenk line, a sample of **1** (1.00 g, 1.02 mmol) was dissolved in dry MeOH (25 mL) and heated to reflux temperatures for 2 h. The solution was transferred back to an argon filled glove box where the reaction mixture was allowed to slowly evaporate until X-ray quality crystals of **4** were isolated.

2.4. Compounds **5**–**7**

The appropriate LaX_3 (X = Cl: 1.00 g, 4.08 mmol; Br: 1.00 g, 2.64 mmol; I: 1.00 g, 1.92 mmol) was dissolved in dry MeOH (~10 mL). After stirring for 10 min, the sample was set aside and the volatile portion was allowed to slowly evaporate until X-ray quality crystals were isolated as: $[LaBr_3(MeOH)_5]$ (**5**) ^{139}La (56.5 MHz, MeOD) $\delta = -34.7$ ppm, $[(MeOH)_4(Cl)_2La(\mu\text{-}Cl)]_2$ (**6**) ^{139}La (56.5 MHz, MeOD) $\delta = -31.2$ ppm, and $[La(MeOH)_9](I)_3\cdot MeOH$ (**7**) ^{139}La (56.5 MHz, MeOD) $\delta = -35.1$ ppm.

2.4.1. Characterization

All analytical data were collected on dried crystalline material. Solution ^{139}La NMR spectra were obtained on a Bruker DRX400 instrument operating at 56.5 MHz using a 5 mm broadband probe with standard single pulse acquisition conditions. The static wide line ^{139}La NMR experiments were performed on a Bruker Avance 400 using 4 mm broadband probe and a solid echo θ–τ–θ-acq sequence using a 1 μs ($\theta = \pi/12$) pulse length, and a inter-pulse spacing $\tau = 20$ μs with 32 K scan averages. Both the solution and solid-state ^{139}La NMR spectra were referenced to an external secondary standard of 1 M $LaCl_3$ ($\delta = 0.0$ ppm). Deconvolutions of line-widths and chemical shifts, along with the simulation of the static second order quadrupolar line shape were performed in software program DMFIT [74].

Standard powder XRD data were collected using a Siemens D500 diffractometer equipped with a diffracted beam graphite monochromator and scintillation detector using 1° incident and diffracted beam slits (diffractometer radius = 250 mm). Scans were collected from 5 to 60° for 2θ, at 0.04° steps, and 2 s count time using CuKα radiation at 40 kV 30 mA. Simultaneous thermogravimetric/differential thermal analysis (TGA/DTA) experiments were performed on an STD 2960 under an atmosphere of argon at a ramp-rate of 5 °C/min to 650 °C.

Information pertaining to the details of the beryllium dome XRD (BeD-XRD) analyses has been previously disseminated [20,75,76]; hence, only a short description is presented here. All sample preparation was performed in an argon filled glovebox using a 1 cm quartz disk (zero-background plate), where the sample was pressed into the specimen cavity, leveled to the holder base using a glass slide, and the BeD cover sealed. The BeD holder was carefully loaded into the Siemens D500 diffractometer. For all scans the instrument settings were 40 kV and 30 mA with a: 0.04° step-size, 1 s count-time, scan range of 5–30° 2θ, 1° divergence and receiving slits; the goniometer radius was 250 mm. Note: Due to the presence of potentially toxic Be^o, it is important that only trained personnel, wearing the appropriate personal protective equipment (i.e., rubber gloves) handle the BeD. If poor handling techniques or any other means shatter the BeD-XRD, proper safety clean-up and disposal protocols must be followed.

2.4.2. General X-ray crystal structure information

Single crystals were mounted onto a glass fiber from a pool of Fluorolube™ and immediately placed in a cold N_2 vapor stream, on a Bruker AXS diffractometer employing an incident-beam graphite monochromator, MoKα radiation ($\lambda = 0.7107$ Å) and a SMART APEX CCD detector. Lattice determination and data collection were carried out using SMART Version 5.054 software. Data reduction was performed using SAINTPLUS Version 6.01 software and corrected for absorption using the SADABS program within the SAINT software package. Structures were solved by direct methods that yielded the heavy atoms, along with a number of the lighter atoms or by using the PATTERSON method, which yielded the heavy atoms. Subsequent Fourier syntheses yielded the remaining light-atom positions. The hydrogen atoms were fixed in positions of ideal geometry and refined using SHELX software. The final refinement of each compound included anisotropic thermal parameters for all non-hydrogen atoms. Table 2 lists the unit cell parameters for the structurally characterized compounds **2**–**7**. All final CIF files were checked using the CHECKCIF program (www.iucr.org/). Additional information concerning the data collection and final structural solutions can be found in the Supplementary data or by accessing CIF files through the Cambridge Crystallographic Data Base. Additional information concerning the data collection and final structural solutions can be found in the CCDC database.

3. Results and discussion

A survey of the crystallographically characterized species [18,19] available with any Ln cation, 3 Br atoms, and any solvent (not water) was undertaken in order to identify potentially useful solvents that would solubilize $LaBr_3$ as well as displace the waters of **1** [20]. Fewer than 30 species met this criteria [55,56,77–87], with the majority being monomers solvated by either THF [78,81,88] or DME [78,80,81]. Additionally, we have isolated a number of solvated LnX_3 species that add to this family, including: $[ScBr_3(THF)_3]$ (**S1**), $[NdBr_3(solv)_4]$ solv = THF (**S2**) and py (**S3**). Data collection parameters for **S1**–**S3** can be found in Table 2, the Supplementary data, and the CCDC database. Of interest for this study were the two compounds directly bound by an ROH, identified as $[NdBr_3(THF)_2(Pr^iOH)_2]$ [55] and $[SmBr_3(Pr^iOH)_4]$ [56] where $Pr^iOH = (CH_3)_2(H)COH$.

For the $LnBr_3(solv)_x$ species, THF has been the most reported solvate crystallized to date; however, in our hands, $LaBr_3$ displayed only limited solubility in THF at room temperature. Alcohols came to the forefront based on a series of solubility experiments with MeOH in particular raising the most interest since LaX_3 readily dissolved in this solvent at room temperature. Structural reports of $[LnX_3(MeOH)_x]$ where the MeOH is directly bound to the Ln metal center have been limited to the Cl [40–46,72,73] derivatives only [18,19]. Due to the void in structurally characterized ROH derivatives of LaX_3, a study concerning the coordination and desolvation behavior of **1** with MeOH was undertaken. It is of note that

Table 2
Data collection parameters for **2**–**7** and **S1**–**S3**.

Compound	**2**	**3**	**4**
Formula	$C_2H_{22}Br_3LaO_9$	$C_6H_{24}Br_2CaO_6$	$C_{10}H_{36}Br_6La_2O_{10}$
Formula weight	568.84	392.15	1075.68
T (K)	173(2)	173(2)	173(2)
Space group	orthorhombic, *Pbca*	hexagonal, *P*-3	monoclinic, *Pc*
a (Å)	12.6540(13)	8.3860(12)	10.1803(16)
b (Å)	12.9686(13)	8.3860(12)	14.794(2)
c (Å)	19.864(2)	6.8655(19)	10.6387(17)
β (°)			106.532(2)
γ (°)		120	
V (Å^3)	3259.7(6)	418.13(14)	1536.0(4)
Z	8	1	2
D_{Calc} (Mg/m^3)	2.318	1.557	2.326
μ (Mo Kα) (mm^{-1})	9.996	5.158	10.581
R1[a] (%) (all data)	1.58 (1.94)	3.99 (4.26)	2.37 (2.57)
wR2[b] (%) (all data)	3.33 (3.44)	10.27 (10.38)	4.94 (5.21)
Compound	**5**	**6**	**7**
Formula	$C_5H_{15}Br_3LaO_5$	$C_8H_{32}Cl_6La_2O_8$	$C_{10}H_{40}I_3LaO_{10}$
Formula weight	533.81	746.86	840.03
T (K)	173(2)	173(2)	173(2)
Space group	orthorhombic, *Pna*2(1)	monoclinic, *P*2(1)/*c*	monoclinic, *P*2(1)/*c*
a (Å)	12.3556(14)	8.750(5)	15.941(3)
b (Å)	9.9655(11)	18.635(11)	8.5737(14)
c (Å)	12.5633(14)	8.278(5)	20.140(3)
β (°)		108.958(8)	93.625(2)
V (Å^3)	1546.9(3)	1276.5(13)	2747.0(8)
Z	4	2	4
D_{Calc} (Mg/m^3)	2.292	1.943	2.031
μ (Mo Kα) (mm^{-1})	10.506	3.954	4.959
R1[a] (%) (all data)	4.58 (4.64)	1.73 (1.75)	1.87 (2.10)
wR2[b] (%) (all data)	11.35 (11.39)	4.35 (4.37)	4.54 (5.52)
Compound	**S1**	**S2**	**S3**
Formula	$C_{12}H_{24}Br_3O_3Sc$	$C_{16}H_{32}Br_3NdO_4$	$C_{20}H_{20}Br_3N_4Nd$
Formula weight	501.00	672.39	700.34
T (K)	181(2)	173(2)	173(2)
Space group	orthorhombic, *Pbcn*	triclinic, *P*-1	orthorhombic, *Pbca*
a (Å)	8.783(3)	8.2662(13)	16.998(2)
b (Å)	13.884(5)	9.3601(15)	17.515(2)
c (Å)	14.540(5)	15.485(2)	32.617(5)
α (°)		79.185(2)	
β (°)		87.106(2)	
γ (°)		74.956(2)	
V (Å^3)	1773.1(11)	1136.5(3)	9711(2)
Z	4	2	16
D_{Calc} (Mg/m^3)	1.877	1.965	1.916
μ (Mo Kα) (mm^{-1})	7.176	7.573	7.088
R1[a] (%) (all data)	0.0967 (0.0986)	0.0463 (0.0505)	0.0386 (0.0866)
wR2[b] (%) (all data)	0.3862 (0.3895)	0.1264 (0.1282)	0.0619 (0.0796)

[a] $R1 = \Sigma \mid |F_o| - |F_c| \mid / \Sigma |F_o| \times 100$
[b] $wR2 = [\Sigma\, w (F_o^2 - F_c^2)^2 / \Sigma (w|F_o|^2)^2]^{1/2} \times 100$

standard analytical characterization methods (i.e., FTIR, ^{1}H and ^{13}C NMR, elemental analysis) for these compounds were of limited utility in identifying these compounds. Of critical importance was single crystal X-ray diffraction and ^{139}La NMR and these results are presented below.

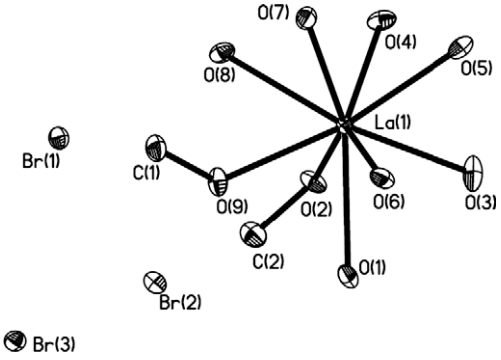

Fig. 2. Structure plot of **2**. Thermal ellipsoids are drawn at 30% level.

3.1. Synthesis of MeOH derivatives

3.1.1. Bromide

After stirring on the bench-top for 12 h, the reaction mixture of **1** in MeOH was set aside with the cap loose to allow any volatile material to slowly evaporate. The resultant X-ray quality crystals proved to be **2**. As can be observed in Fig. 2, the original dimer of **1** (Fig. 1a) was disrupted upon introduction of MeOH, forming a 3OS monomer. For **2**, the La metal center maintains its 9 coordination through the binding of the original 7 H_2O molecules with 2 additional MeOH solvent molecules. Due to the increased steric bulk of the MeOH in comparison to the waters, coupled with the increased number of electron donating oxygen atoms around the La metal center, all of the Br atoms are forced to the outersphere. Since the 3OS structure (Fig. 1c) of $LnBr_3$ has previously been

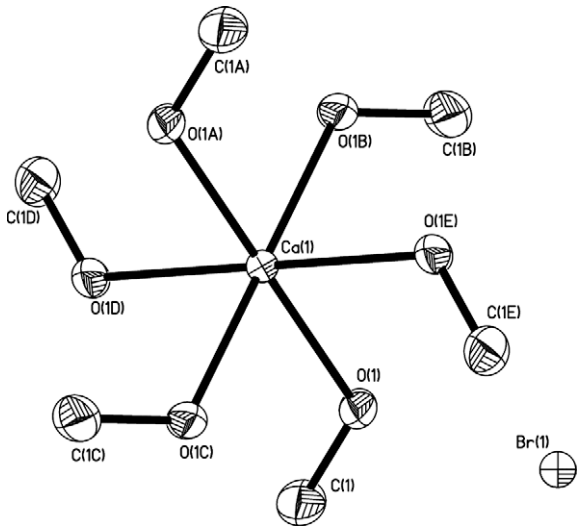

Fig. 3. Structure plot of **3**. Thermal ellipsoids are drawn at 30% level. The missing mirror reflected Br is not shown.

observed only for the smaller heavier Ln anions or for the $LnI_3{\cdot}n$-H_2O derivatives, an appropriate structural model is not readily available [20–36]. The Ln–O distances of **2** (av. 2.55 Å for H_2O and av. 2.53 Å MeOH) were found to be in agreement with **4** and **5** (see Table 2) and the hydrates (av. 2.55 Å for $LaBr_3{\cdot}n\ H_2O$) [20], but significantly longer than the literature alcohol derivatives (av. 2.46 Å [55,56]).

Several attempts to employ in situ drying agents to remove the water ligands of **1** upon dissolution in MeOH were investigated. In one of these studies, the crystal isolated from the dissolution of **1** in MeOH in the presence of CaH_2 (the drying agent employed) proved to be the Ca derivative **3**, not the desired La species. For **3**, the Ca atom is octahedrally bound by MeOH with 2 outersphere Br atoms present in the lattice. Since no $CaX_2{\cdot}n$MeOH species have been previously presented [18,19], it is reported here and shown in Fig. 3. The alkaline earth was apparently more halophilic than the lanthanide with a calculated by-product being 2/3 "LaH_3". All other attempts to isolate hydrate free LnX_3 species at room temperature through drying agents were not successful.

Therefore, higher temperature processes were investigated, without the drying agent additives. Compound **1** was heated in MeOH at reflux temperatures for 2 h under an argon atmosphere. After cooling to room temperature and vacuum distillation of the majority of the reaction's volatile component, X-ray quality crystals were isolated that proved to be **4** (Fig. 4). The bound waters were successfully replaced by MeOH but an unusual salt structure was formed instead of the simple coordination species previously reported for ROH derivatives [18,19,40–46,55,56,72,73]. In **4**, the 9-coordinated La cation of the first molecule in the unit cell was modeled with 2.75 Br atoms and 5.25 MeOH solvent molecules for an overall +0.25 charge. One of the Br sites (Br7) was partially occupied by an oxygen atom from a MeOH ligand and was refined for the Br:O ratio at 0.75:0.25. A partially occupied methyl carbon atom was also observed coordinated to the disordered O site and was constrained to have the same 0.25 occupancy. The other 9-coordinated La cation in the unit cell was modeled to have 3.25 Br atoms and 4.75 MeOH solvent molecules for an overall −0.25 charge. Again, a coordinated MeOH (O3) was found to partially occupy one of the Br sites at a Br:O ratio of 0.25:0.75. An additional methyl carbon (C3) was located near O3 atom position and constrained to have the same 0.75 occupancy.

The metrical data for **2** and **4** are listed in Table 3. Due to the substantial differences in the two structures, the Ln–solv distances and angles are the only comparable metrical data. The fully solvated La cation of **2** has substantially longer Ln–solv distances than that of the salt **4**. This must be a reflection of the electron withdrawing strength of the bound halides in **4** and the increased electron donation by the increased number of bound ROH and H_2O molecules in **2**.

Due to the surprising complexity of **4**, it was of interest to determine the coordination behavior of anhydrous $LaBr_3$ [20] in MeOH. X-ray quality crystals were successfully grown by slow evaporation of the reaction mixture under an argon atmosphere. The 8-coordinated La metal center of **5** (see Fig. 5) is best considered distorted square antiprism using 3IS Br atoms and 5 MeOH solvent molecules to fill the coordination sites. The formation of the 3IS structure of **5** versus the 3OS of **2** must be due to the steric bulk of the MeOH preventing the binding of additional solvent ligands that would electronically satisfy the La; thereby, forcing the Br anions to the outersphere. The only other structures of ROH/Ln/3 Br derivatives reported [18,19] are the previously discussed monomeric Pr^iOH derivatives[55,56]. For **5** the Ln–Br and Ln–ROH distances (3.00 and 2.53 Å), respectively, are elongated when compared to the $[NdBr_3(THF)_2(Pr^iOH)_2]$ [55] (2.85 and 2.46 Å) and $[SmBr_3(Pr^iOH)_4]$ [56] (2.83 and 2.46 Å). This variation is most likely a result of the additional electron donation by the 5 MeOH ligands in comparison to the 4 Lewis bases on the other compounds.

Due to the similar make up of **4** and **5**, it was of interest to elucidate the conditions that yielded the particular structure. From a sealed capillary tube containing a concentrated solution of $LaBr_3$ dissolved in MeOH, crystals that proved to be **4** were isolated. This led us to investigate the role that concentration played in the final structure observed. Crystals of **4** were also successfully isolated from a super saturated solution of $LaBr_3{\cdot}n$MeOH (i.e., the reaction mixture had to be heated to generate a clear solution). In contrast,

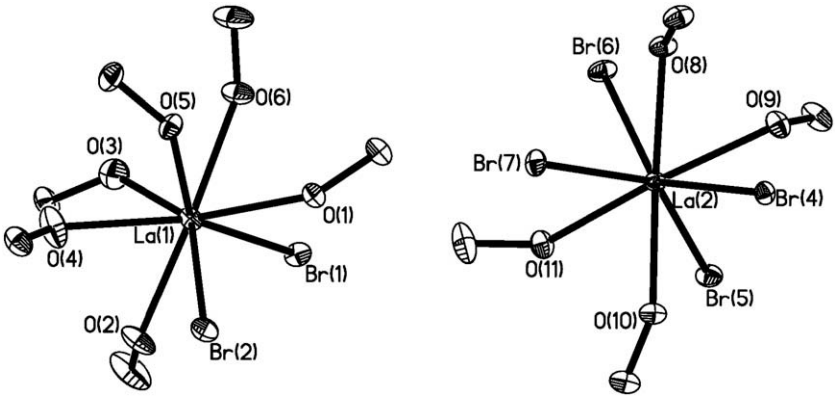

Fig. 4. Structure plot of **4**. Thermal ellipsoids are drawn at 30% level.

Table 3
Metrical data for **2**, **4** – **7**.

Compound	Ln–X (Å)	Ln–X (Å)	Ln–(μX) (Å)	Ln–solv (Å)	X–La–X (°)	X–La–solv (°)	solv–La–solv (°)
2		5.21–14.18		2.55 (H_2O) 2.53 (MeOH)			66.6–142.3
4	2.98			2.46	86.3–145.3	82.4–145.8	82.4–145.8
5	3.00			2.56	102.9–146.4	68.5–146.7	68.1–142.1
6	2.86		2.865	2.53	78.9–141.6	69.2–145.7	71.7–142.8
7		5.28–13.16		2.55 av			66.0–139.4

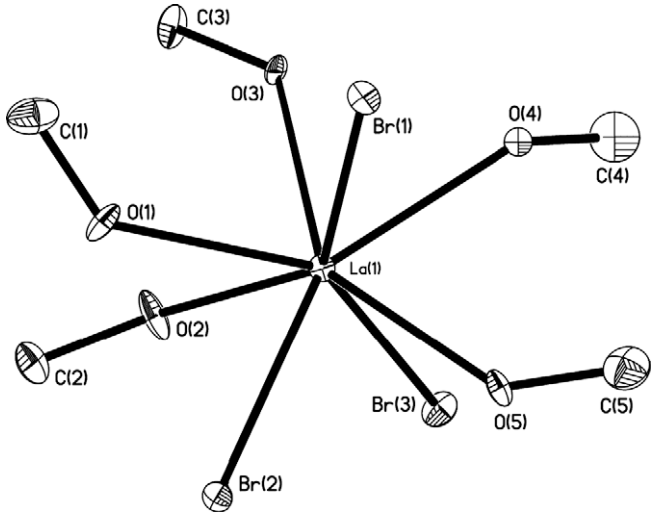

Fig. 5. Structure plot of **5**. Thermal ellipsoids are drawn at 30% level.

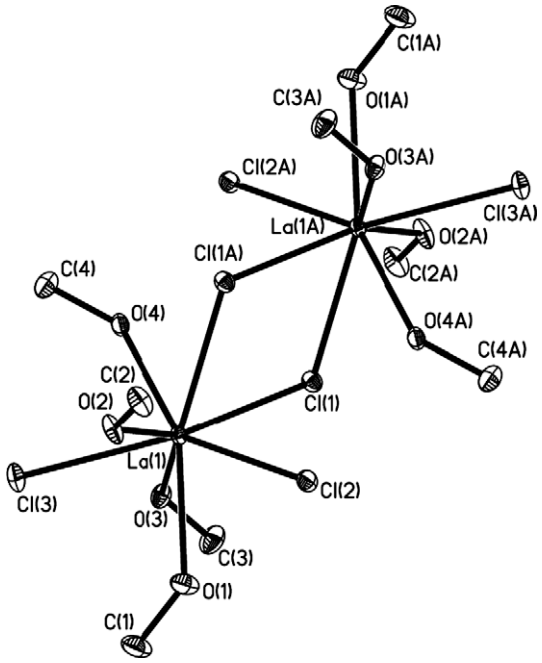

Fig. 6. Structure plot of **6**. Thermal ellipsoids are drawn at 30% level.

a very diluted solution of **1** refluxed in MeOH that was allowed to slowly evaporate yielded crystals of **5**. From these reactions, compounds **4** and **5** were isolated from the same reaction mixtures that had previously yielded the other structure. Therefore, rapid crystal growth at high concentrations appears to lead to the disordered salt **4** and longer slower growth yields the monomeric neutral species **5**.

3.1.2. Chloride

Based on the significant changes noted for the Br derivatives, in comparison to literature compounds [18–20,55,56], it became of interest to understand how the other halide structures would be affected by MeOH substitution. A search of the structure literature concerning compounds with any Ln cation, 3 Cl or I anions, and any solvent (not water) was again undertaken [18,19]. In contrast to the small number of compounds found for the 'Ln/3Br/solvate' structure search, more than 230 solvated compounds were available that contained three Cl atoms for each Ln center [18,19]. The majority of these compounds were found to be monomers, using pyridine *n*-oxide, polyamines, crown ethers, phosphine oxides, pyrazolyl borates, dimethoxyethane, acetonitrile, ROHs, and other simple organic solvents. Of the ROH derivatives bound to the Ln cation, only eight compounds were with MeOH [40–46,72,73] and four with ethanol (EtOH) [47–50]; however, these structures were isolated in the presence of other co-ligands such as crown ethers [44,45,47,48] or polypyridyl [40–43,49]. The one exception was the previously discussed $[Ce(\mu\text{-}Cl)Cl_2(MeOH)_4]_2$ [72,73]. Three Ln compounds bound by Pr^iOH, $[(Pr^iOH)_3(Cl)_2Ln(\mu\text{-}Cl)]_2$ where Ln = La [51], Ce [52], Nd [53] (similar to the Yb/THF [89] species), and one *n*-butanol bound Tb salt $[TbCl_5(HO(CH_2)_3CH_3](HNC_5H_4\text{-}Me\text{-}2)$ [54] have also been disseminated.

Due to the limited information on MeOH systems of the LaX_3 congeners, a dried sample of $LaCl_3$ that had been prepared according to Eq. (1) [20] was dissolved in MeOH. After stirring for 24 h, X-ray quality crystals were grown over an extended period of time by slow evaporation of the volatile portion of the reaction mixture. The Cl derivative **6** was solved as the dinuclear species (see Fig. 6) where each 8-coordinated La possesses 3IS Cl atoms (two terminal and one bridging) and four MeOH solvent molecules filling the rest of the coordination sphere. This is a similar construct as predicted more than 40 years ago by Smith et al. [90] and observed for the congener $[(MeOH)_4(Cl)_2Ce(\mu\text{-}Cl)]_2$ [72,73], as well as the

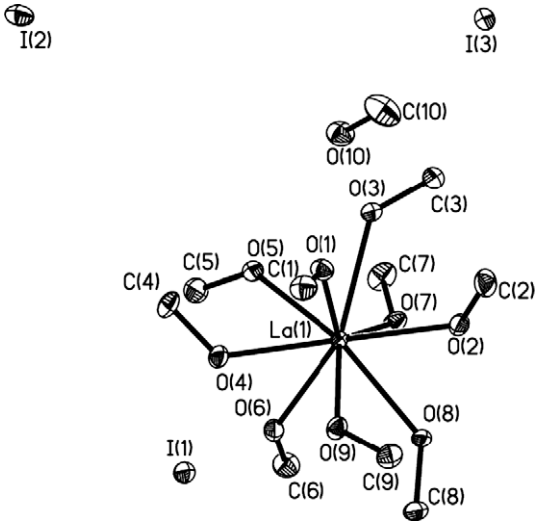

Fig. 7. Structure plot of **7**. Thermal ellipsoids are drawn at 30% level.

Pr^iOH derivatives: $[(Pr^iOH)_3(Cl)_2Ln(\mu\text{-}Cl)]_2$ where Ln = La [51], Ce [52], Nd [53]. The La–ROH (2.53 Å), La–Cl(2.86 Å), and La(μ-Cl) (2.87 Å) distances of the chloride derivative **6** were consistent with the $[(MeOH)_4(Cl)_2Ce(\mu\text{-}Cl)]_2$ [72,73] when the cation size is taken into account but varied in comparison to $[(Pr^iOH)_3(Cl)_2La(\mu\text{-}Cl)]_2$ (av La: -ROH 2.52 Å; -Cl 2.78 Å; -μ-Cl 2.96 Å). [51] The (μ-Cl)–La–(μ-Cl) and La–(μ-Cl)–La bond angles (78.9 and 141.6° for **6** versus 72.0 and 108.0° for $[(Pr^iOH)_3(Cl)_2La(\mu\text{-}Cl)]_2$ [51]) were not found to be in agreement, which was attributed to the additional MeOH around the 8-coordinated La of **6** versus the 7-coordinated La of the Pr^iOH structures [51–53].

3.1.3. Iodide

For the reported structures [18,19] that possess one Ln, three I, and non-aqueous solvate, more than 55 structures met the desired criteria [38–40,83,91–116]. While these complexes ranged in nuclearity, the majority were monomers adopting a 2IS/1OS arrangement $[(L)_xLnI_2](I)$ [38,40,91–96,106,111,117] (where L = neutral ligand or organic solvents such as: Pr^iOH [38], THF [106,117], and py [38,106]) or the 3IS arrangement that utilizes combinations of bulky neutral ligands [83,95,107,110,114,118], THF [98,100,102,113], or Pr^iOH [39] to fill the coordination sphere. However, no structure reports of the LaI_3·MeOH derivatives have been previously reported.

De-hydrated LaI_3 (Eq. (1)) [20] was dissolved in MeOH and X-ray quality crystals grown as noted above. The crystal solved as **7** (see Fig. 7) in a 3OS arrangement for the halides, 9 MeOH solvent molecules bound to the La metal center, and an additional MeOH located in the unit cell lattice. The coordination around the metal center is in direct contrast with the literature reported ROH derivatives $[LnI_3(Pr^iOH)_4]$ [39] (Ln = Ce, La) and $[LuI_2(Pr^iOH)_4](I)$ [38]. None of these compounds are reasonable models and as a result the La–ROH distances of **7** (av 2.55 Å) were found to be longer in comparison: 2.238–2.271 Å (Lu) [38], 2.492–2.524 Å (La), and 2.478–2.496 Å (Ce) [38,39]. A better structural model is $[La(H_2O)_9](I)_3$ [20] where the Ln–H_2O (av 2.54 Å) and Ln–I distances (range 5.13–6.81 Å) were found to be in line with those noted for **7** (Ln–I = 5.28 Å).

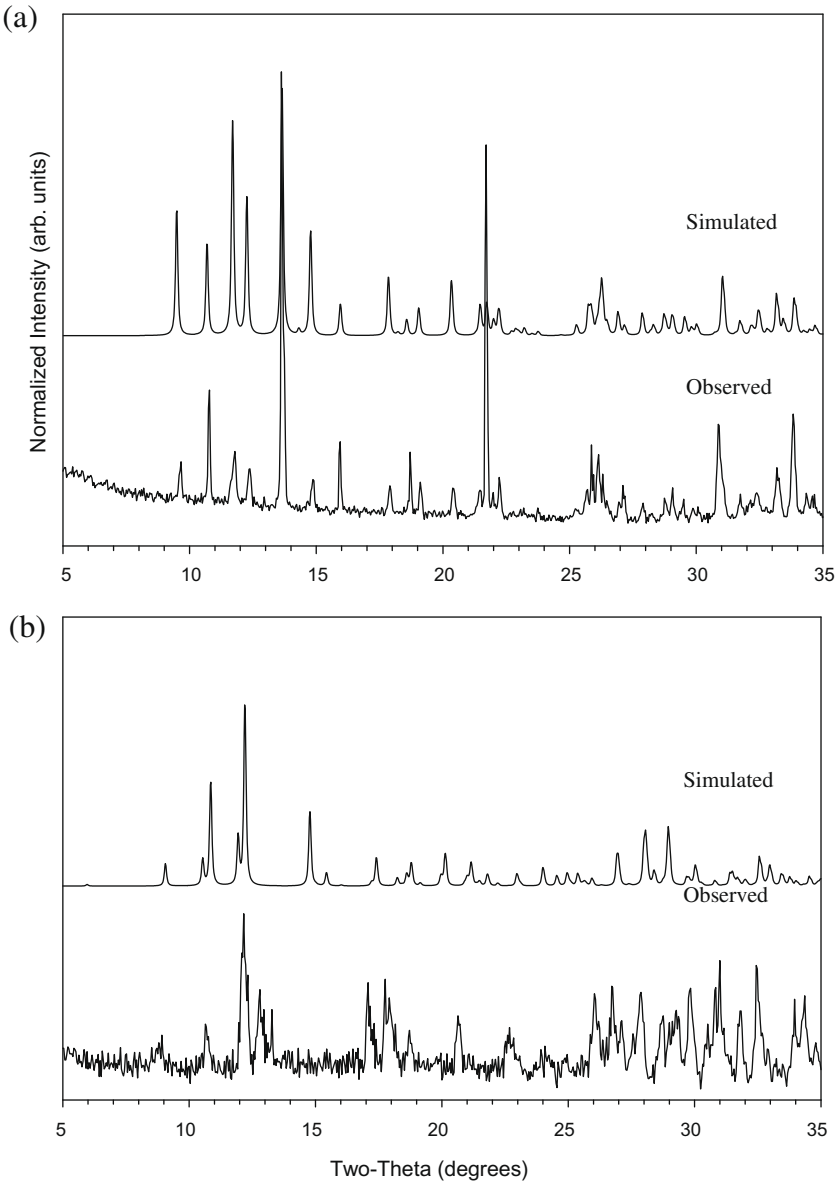

Fig. 8. BeD–XRD patterns (calculated and experimental) of (a) **6** and (b) **5**.

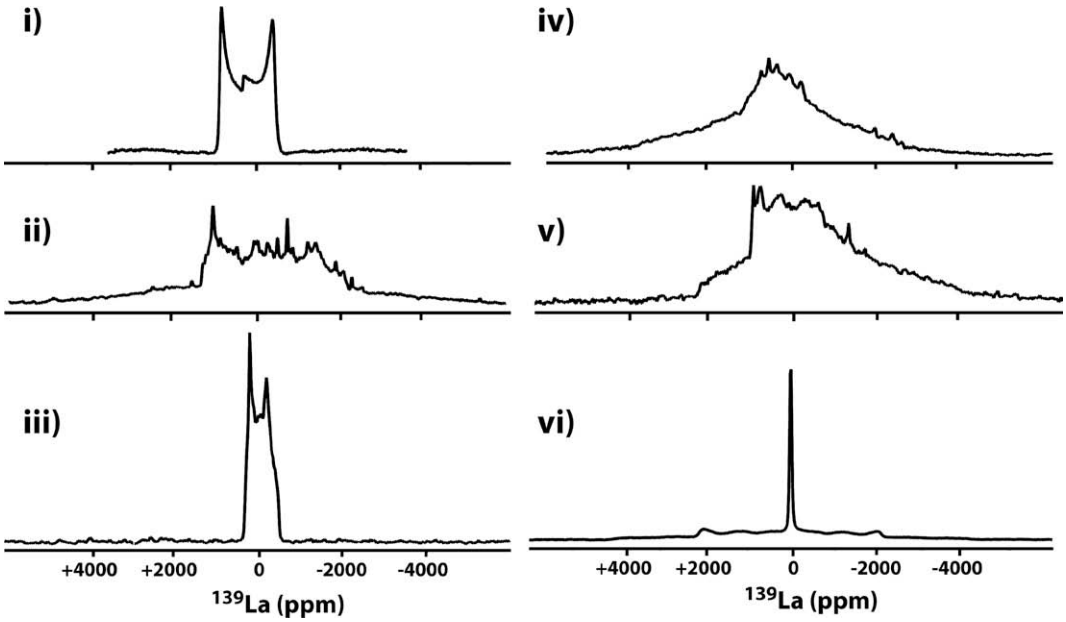

Fig. 9. Solid-state ^{139}La NMR data for: (i) $LaBr_3$, (ii) **1**, (iii) **2**, (iv) **5**, (v) **6**, (vi) **7**.

3.1.4. Bulk powder characterization

The limitations of standard analytical methodologies in supplying useful data concerning the bulk $LnX_3(MeOH)_x$ products led us to investigate alternative characterization techniques such as beryllium dome PXRD (BeD XRD) which is a useful method for characterizing air-sensitive species [20,75,76]. The BeD–XRD patterns were obtained for **4**–**7** (Fig. 8) and were compared to the simulated powder X-ray patterns generated from the solved single crystal structure. The patterns obtained for **6** (Fig. 8a) were found to be consistent with the theoretical patterns. Variability of the observed peak intensities results from texture effects and large grains present in the bulk powder versus the assumed randomize powders for the calculated patterns. For **5** and **7** the PXRD patterns observed were not consistent with the simulated pattern. For **5** (Fig. 8b) in addition to the expected pattern, the experimental data also reveals some additional peaks, which have been tentatively assigned to partially desolvated species of **5** (i.e., −1 MeOH, −2 MeOH, etc). The patterns noted for **7** were broad and indistinct and no direct comparison can be made.

Since the BeD–XRD data yielded limited information on the characterization of the bulk powder, solid-state ^{139}La NMR experiments were undertaken and spectra obtained for $LaBr_3$ [20], **1** [20], **2** and **5** (Fig. 9). The ^{139}La nucleus has a 7/2 spin nucleus with considerable quadrupolar interaction and possesses a quadrupolar coupling constant (QCC) that is predicted to be between 15 and 30 MHz. These properties lead to broad, second order, quadrupolar line shapes, which are very sensitive to the local bonding symmetry surround the La nucleus.

For $LaBr_3$, simulation (Fig. 9i) of the quadrupolar lineshape gave QCC = 17.4 MHz, an asymmetry parameter of $\eta = 0$ and an isotropic chemical shift of $\delta_{iso} = 418$ ppm [20]. This is consistent with previous literature reports for $LaBr_3$ (QCC = 17 MHz, $\eta = 0$ and $\delta_{iso} = 400$ ppm) [119]. A chemical shielding anisotropy (CSA) of ~100 ppm has also been reported [119] but makes only a minor impact on the NMR spectrum at this moderate magnetic field strength. The symmetric electric-field gradient (EFG) tensor ($\eta = 0$) reflects the symmetry around the La that resides on a single crystallographic site with C_3 symmetry and is equivalent to that observed in $LaCl_3$ [119]. The chemical shift for $LaBr_3$ ($\delta_{iso} = +418$ ppm) is less shielded than that reported for $LaCl_3$ ($\delta_{iso} = +305$ ppm) or LaF_3 ($\delta_{iso} = -135$ ppm) and reflects a strong inverse-halogen dependence within these La-trihalides.

The addition of water within these compounds modifies the local structure resulting in the removal of the local La nucleus symmetry. For example, $LaCl_3{\cdot}6H_2O$ shows a dramatic increase in both the quadrupolar coupling constant and asymmetry of the ^{139}La EFG tensor, QCC = 23.7 MHz, with $\eta = 0.40$, in comparison to $LaCl_3$, QCC = 15.3–15.5 MHz, $\eta = 0.00$ [119,120]. For compound **1** (Fig. 9ii) the ^{139}La NMR data gave QCC = 25.3 MHz, $\eta = 0.39$ with $\delta_{iso} = +315$ ppm reflecting the loss of local symmetry to the La environment. The reduction in the chemical shift of **1** compared to the observed chemical shift of $LaBr_3$ ($\delta_{iso} = +418$) reflects the incorporation of oxygen into the coordination environment. This also demonstrates that the La is not fully coordinated by oxygen atoms alone, which would have a chemical shift between +200 and −200 ppm [121]. While the general breadth of the observed ^{139}La spectrum is consistent with incorporation of water into the La coordination environment, the "irregular spikes" observed in the spectrum argues that a range of La environments exist [20]. Similar spikes have been reported for the LaI_3 material and in that case were attributed to samples that formed fibrous mats and did not reflect true powder samples [119].

In contrast to the spectra of **1**, the mixed solvate species **2** yielded a much narrower ^{139}La NMR spectrum (Fig. 9iii) with QCC = 11.8 MHz, $\eta = 0.39$ and $\delta_{iso} = +16.9$ ppm. The reduction in the QCC is consistent with the very similar La–O bond distances in the coordinating H_2O (2.55 Å) and MeOH (2.53 Å) ligands (see Table 2). The dramatic reduction in the chemical shift reflects the increased shielding around the La nuclei, and also demonstrates that the Br nuclei are not directly bonded to the La as observed in the reported structure (Table 2 and Fig. 2). For compounds with only oxygen-bearing ligands a correlation between La coordination number (CN) and the isotropic chemical shift has been proposed [121]. Based on this correlation the $\delta_{iso} = +16.9$ ppm corresponds to a CN = 9–10, consistent with the structure (Fig. 2).

The exceptionally broad ^{139}La NMR spectra of **5** and **6** do not allow for a unique determination of the EFG tensor values but the very large widths do reflect a loss of symmetry around the La nucleus. These spectra are consistent with structures that the possesses 3 coordinating halide atoms and a number of coordinating

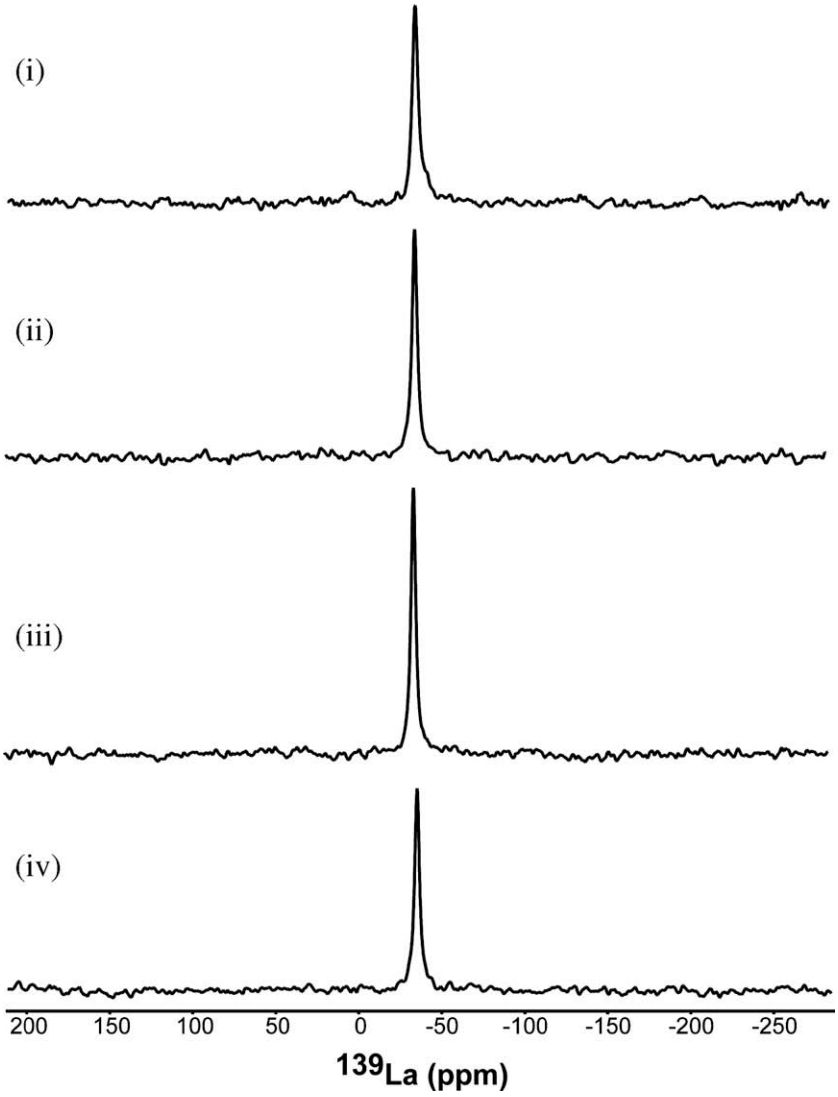

Fig. 10. Solution (MeOD) ^{139}La NMR data for (i) **2** (δ ^{139}La = −32.7), (ii) **5** (δ ^{139}La = −34.7), (iii) **6** (δ ^{139}La = −31.2), (iv) **7** (δ ^{139}La = −35.1).

oxygen nuclei from MeOH. Therefore, it is apparent that the solid state spectra are consistent with the solid state structures of **5** and **6**. For **7**, the sharp singlet is consistent with the 3OS structure where the nuclei are symmetrically coordinated by MeOH and no broadening is noted since the halides are located in the outersphere.

3.1.5. Solution characterization

Further characterization of **2**, **5**–**7** in MeOD was undertaken using NMR spectroscopic investigations. Due to the limited information that could be garnered by standard NMR nuclei (i.e., ^{1}H, ^{13}C), solution ^{139}La NMR spectra were collected (see Fig. 10). The similarity of the observed chemical shifts (δ_{iso} from −31 to −35 ppm) coupled with the large change from the δ_{iso} measured by solid state ^{139}La NMR for **2** and **5** (vide infra), clearly demonstrates that the structures are not retained in solution. The range of δ_{iso} is consistent with oxygen only coordinating ligands where each La has a CN ~10. This chemical shift (−34 to −40 ppm) has been previously attributed to the fully hydrated La sites within zeolites [120,122]. Based on these data, it is reasoned that in MeOH, compounds **2**, **5**–**7** adopt a 3OS geometry with the nuclei fully solvated by O bearing solvents (i.e., MeOH or H_2O).

3.1.6. Thermal decomposition

Since there were significant structural variations noted between the hydrated species (Fig. 1) and the methanolated compounds **5**-**7** (Figs. 5-7), the thermal desolvation temperatures of these MeOH derivatives were investigated. A review of the TGA/DTA data on the dimer $LnX_3{\cdot}nH_2O$ (X = Cl and Br) species, revealed that there were at least three weight loss steps accompanied by three endotherms initiating/ending at 75/175 °C and 100/225 °C, respectively. In contrast, the I derivative (3OS – Fig. 1c) showed only one weight loss and a fairly flat thermal event over this temperature range [20].

Under identical conditions noted for the hydrates, the TGA/DTA spectra of **5**-**7** were obtained (see Fig. 11i–iii, respectively). The TGA weight loss for full MeOH removal for **5**, **6**, and **7** were calculated to be 34.3, 30.0 and 38.1%, respectively and are consistent with the experimentally obtained weight losses achieved at 250 °C. Additional weight losses noted in the TGA spectra at higher temperatures are associated with halide volatility, as observed for the hydrate system [20]. For **5** (Fig. 11i), the de-solvation of the 3IS Br adduct initiates at 100 °C and is complete by 200 °C, following multiple weight loss steps and numerous endotherms. Not unexpected, this pattern is similar to the spectrum obtained for the *iso*-structural $[(H_2O)_6Br_2Ce(\mu\text{-}Br)]_2$ [20]. The overall spectrum of

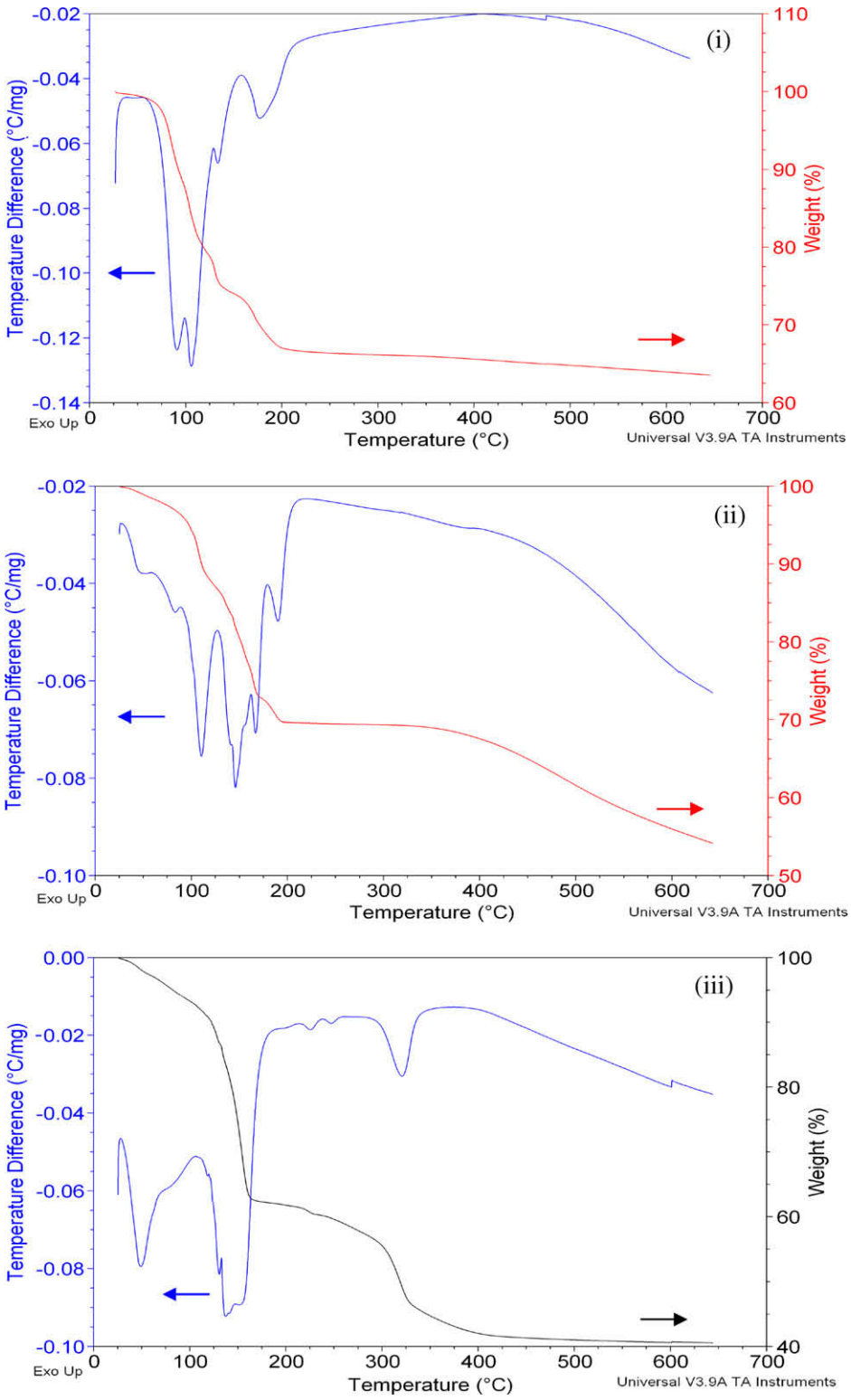

Fig. 11. TGA/DTA spectrum of (i) **5**, (ii) **6**, (iii) **7**.

the Cl derivative, **6** is also nearly identical to its *iso*-structural hydrate spectrum, with multiple weight loss steps initiated between 75 to 180 °C coupled to three major and one minor endotherm. For **7**, three distinct weight losses with three separate endotherms were noted for the two weight loss steps. This is surprisingly different from the *iso*-structural 3OS hydrate spectrum. Combined, the de-methanolation appears complete at ~200 for **5** and **6** but 155 °C for **7**, which are slightly elevated in comparison to the hydrate species.

4. Summary and conclusion

Attempts to dehydrate **1** through room temperature dissolution in MeOH led to the crystallographic characterization of **2**, a 3OS

anion species with the La metal center coordinated by a mixture of H_2O and MeOH solvate ligands. An unusual salt derivative (**4**) was isolated from a heated reaction mixture of **1** in MeOH. Each La metal center is 8-coordinated using MeOH and Br atoms but the distribution of the Br atoms is not equal between the two metal centers. In contrast, the first structural derivatives of LaX_3 solvated by MeOH were synthesized from the dissolution of the anhydrous LaX_3 in MeOH, which have been identified as 8-coordinated species: **5**, a monomer using five MeOH and 3IS bromide anions; **6**, a dimer with full IS chloride anions (four terminal and two bridging) and MeOH solvate ligands; **7**, a monomer with 3OS iodide anions and 8 MeOH ligands. Solution structures were determined by ^{139}La NMR studies to be 3OS for **5**–**7**. While structural changes were produced by the solvent exchange, in comparison to the water derivatives, the thermal decomposition of the MeOH derivatives (**5**–**7**) appeared to be very similar or require higher temperatures than the hydrates. Alternative ROH and non-ROH based solvent systems are being explored as a means to generate LaX_3 at lower processing temperatures.

Acknowledgments

For support of this research, the authors thank the Department of Homeland Security, the National Institutes of Health funded through the NIH Roadmap for Medical Research, Grant #1 R21 EB005365-01 [information on this RFA (Innovation in Molecular Imaging Probes) can be found at http://grants.nih.gov/grants/guide/rfa-files/RFA-RM-04-021.html], and the US Department of Energy, Office of Basic Energy Sciences, Division of Materials Sciences and Engineering under Contract DE-AC04-94AL85000. Sandia is a multiprogramming laboratory operated by Sandia Corporation, a Lockheed Martin Company, for the United States Department of Energy.

Appendix A. Supplementary data

CCDC 714429–714434 and 730384–730386 contain the supplementary crystallographic data for complex **2**–**7** and **S1**–**S3**, respectively. These data can be obtained free of charge via www.ccdc.cam.ac.uk/conts/retrieving.html, or from the Cambridge Crystallographic Data Centre, 12 Union Road, Cambridge CB2 1EZ, UK; fax: (+44) 1223 336 033; or e-mail: deposit@ccdc.cam.ac.uk. Supplementary data associated with this article can be found, in the online version, at doi:10.1016/j.poly.2010.02.027.

References

[1] W.W. Moses, Nucl. Instrum. Methods Phys. Res., Sect. A 287 (2002) 123.
[2] K.W. Kramer, P. Dorenbos, H.U. Gudel, C.W.E. van Eijk, J. Mater. Chem. 21 (2006) 2773.
[3] P. Dorenbos, Phys. Status Solidi A 202 (2005) 195.
[4] R. Carchon, M. Moeslinger, L. Bourva, C. Bass, M. Zendel, in: 11th Symposium on Radiation Measurements and Applications, Univ Michigan, Ann Arbor, MI, Aug. 21, 2007, Nucl. Instrum. Methods Phys. Res., Sect. A: Univ Michigan, Ann Arbor, MI, 2006, pp 380-383.
[5] M.J. Hamson, F.P. Doty, Conference on Penetrating Radiation Systems and Applications VIII, San Diego, CA, Proc. Soc. Photo-Opt. Inst. Eng. (SPIE), San Diego, CA, 2007, pp B7070–B7070.
[6] F.P. Doty, D. McGregor, M. Harrison, K. Findley, R. Polichar, Conference on Penetrating Radiation Systems and Applications VIII, San Diego, CA, Proc. Soc. Photo-Opt. Inst. Eng. (SPIE): San Diego, CA, 2007, p 70705.
[7] W.W. Moses, K.S. Shah, in: Proceedings of the seventh International Conference on Inorganic Scintillators and Industrial Applications, Nucl. Instrum. Methods Phys. Res., Sect. A: Sept. 8–12, 2003, pp 317–320.
[8] P. Yang, C.B. DiAntonio, T.J. Boyle, M.A. Rodriguez, M.R. Sanchez, Penetrating Radiation Systems and Applications VIII Conference Proceedings, San Diego, CA, SPIE Optics + Photonics 07: San Diego, CA, 2007, p. 670709.
[9] W.W. Wendlandt, J. Inorg. Nucl. Chem. 5 (1957) 118.
[10] M.D. Taylor, C.P. Carter, J. Inorg. Nucl. Chem. 24 (1962) 387.
[11] T. Balaji, S. Buddhudu, Mater. Chem. Phys. 34 (1993) 310.
[12] G. Meyer, T. Staffel, Z. Anorg. Allg. Chem. 352 (1986) 31.
[13] F.H. Spedding, J.P. Flynn, J. Am. Chem. Soc. 76 (1954) 1474.
[14] F.H. Spedding, C.F. Miller, J. Am. Chem. Soc. 74 (1951) 4195.
[15] A. Habenschuss, F.H. Spedding, J. Chem. Phys. 70 (1979) 2797.
[16] A. Habenschuss, F.H. Spedding, J. Chem. Phys. 70 (1979) 3758.
[17] G. Meyer, L.R. Morss, Synthesis of Lanthanide and Actinide Compounds, Kluwer Academic Publishers, Boston, 1991.
[18] CONQUEST Version 1.10, Cambridge Crystallographic Data Centre:support@ccdc.cam.ac.uk or www.ccdc.cam.ac.uk (V 5.30 NOV 2008). In CONQUEST Version 1.10, Cambridge Crystallographic Data Centre:support@ccdc.cam.ac.uk or www.ccdc.cam.ac.uk (V 5.30 NOV 2008).
[19] F.H. Allen, Acta Crystallogr., Sect. B 58 (2002) 380.
[20] T.J. Boyle, P. Yang, L.A.M. Ottley, M.A. Rodriguez, T.M. Alam, S. Hoppe, Unpublished work (2009).
[21] C.J. Kepert, B.W. Skelton, A.H. White, Aust. J. Chem. 47 (1994) 385.
[22] E.J. Peterson, E.I. Onstott, R.B. Von Dreele, Acta Crystallogr., Sect. B (1979) 805.
[23] A. Habenschuss, F.H. Spedding, Cryst. Struct. Commun. 7 (1978) 535.
[24] A. Habenschuss, F.H. Spedding, Cryst. Struct. Commun. 9 (1980) 71.
[25] D.L. Kepert, J.M. Patrick, A.H. White, Aust. J. Chem. 36 (1983) 477.
[26] M. Marezio, H.A. Plettinger, W.H. Zachariasen, Acta Crystallogr., Sect. 3514 (1961) 234.
[27] A.M.T. Bell, A.J. Smith, Acta Crystallogr., Sect. C 46 (1990) 960.
[28] R.D. Rogers, L.K. Kurihara, Lanthanide Actinide Res 1 (1986) 296.
[29] A. Habenschuss, F.H. Spedding, Cryst. Struct. Commun. 9 (1980) 157.
[30] A. Habenschuss, F.H. Spedding, Cryst. Struct. Commun. 9 (1980) 207.
[31] A. Habenschuss, F.H. Spedding, Cryst. Struct. Commun. 9 (1980) 213.
[32] A. Habenschuss, F.H. Spedding, J. Chem. Phys. 73 (1980) 442.
[33] J. Chen, D. Xu, L. Li, J. Wu, G. Xu, Acta Crystallogr., Sect. C 47 (1991) 1074.
[34] P.C. Junk, L.I. Semenova, B.W. Skelton, A.H. White, Aust. J. Chem. 52 (1999) 531.
[35] K.C. Lim, B.W. Skelton, A.H. White, Aust. J. Chem. 53 (2000) 875.
[36] K.C. Lim, B.W. Skelton, A.H. White, Aust. J. Chem. 53 (2000) 867.
[37] F.A. Cotton, G. Wilkinson, Advanced Inorganic Chemistry, fifth edition., John Wiley & Sons, New York, 1988.
[38] G.R. Giesbrecht, J.C. Gordon, D.L. Clark, B.L. Scott, Inorg. Chem. 43 (2004) 1065.
[39] D.M. Barnhart, T.M. Frankcom, P.L. Gordon, N.N. Sauer, J.A. Thompson, J.G. Watkin, Inorg. Chem. 34 (1995) 4862.
[40] F. Bravard, Y. Bretonniere, R. Wietzke, C. Gateau, M. Mazzanti, P. Delangle, J. Pecaut, Inorg. Chem. 42 (2003) 7978.
[41] U.P. Singh, R. Kumar, J. Mol. Struct. 837 (2007) 214.
[42] R. Wietzke, M. Mazzanti, J.-M. Latour, J. Pecaut, P.-Y. Cordier, C. Madic, Inorg. Chem. 37 (1998) 6690.
[43] R. Wietzke, M. Mazzanti, J.-M. Latour, J. Pecaut, Inorg. Chem. 38 (1999) 3581.
[44] G. Crisci, G. Meyer, CCDC Private Communication (2001).
[45] R.D. Rogers, L. Nunez, Inorg. Chim. Acta 172 (1990) 173.
[46] J.-G. Mao, Z.-S. Jin, J.-Z. Ni, Jiegou Huaxue 13 (1994) 377.
[47] E. Forsellini, F. Benetollo, G.D. Paoli, G. Bombieri, Euro. Cryst. Meeting 7 (1982) 211.
[48] E. Forsellini, F. Benetollo, G. Bombieri, A. Cassol, G.D. Paoli, Inorg. Chim. Acta 109 (1985) 167.
[49] J. Hallfeldt, W. Urland, Z. Anorg. Allg. Chem. 627 (2001) 545.
[50] L.I. Semenova, B.W. Skelton, A.H. White, Aust. J. Chem. 52 (1999) 551.
[51] A.I. Yanovsky, Z.A. Starikova, E.P. Turevskaya, N.Y. Turova, A.P. Pisarevsky, Y.T. Struchkov, Zh. Neorg. Khim. 41 (1996) 1248.
[52] M. Schafer, R. Herbst-Irmer, U. Groth, T. Kohler, Acta Crystallogr., Sect. C 50 (1994) 1256.
[53] J. Zhongsheng, W. Shenglong, W. Fusong, S. Cheng, Y. Guangdi, F. Yuguo, Chem. J. Chin. Univ. 6 (1985) 735.
[54] W. Urland, J. Hallfeldt, Z. Anorg. Allg. Chem. 626 (2000) 2569.
[55] H.Y.S. Chun, H. Huang, G.X. Xu, Z.S. Ma, N.-C. Shi, Chin. Chem. Lett. 5 (1994) 255.
[56] L.E. Depero, M.T. Arienti, M. Zocchi, M.C. Gallazzi, Struct. Chem. 2 (1991) 595.
[57] R. Kumar, U.P. Singh, J. Mol. Struct. 875 (2008) 427.
[58] Y.-Q. Liu, X.-R. Zeng, L.-P. Lei, Acta Crystallogr., Sect. E (2007) M2695.
[59] Q. Chen, Y.D. Chang, J. Zubieta, Inorg. Chim. Acta 258 (1997) 257.
[60] R.D. Rogers, A.N. Rollins, M.M. Benning, Inorg. Chem. 27 (1998) 3826.
[61] M. Albrecht, S. Mirtschin, O. Osetska, S. Dehn, D. Enders, R. Frohlich, T. Pape, E.F. Hahn, Eur. J. Inorg. Chem. (2007) 3276.
[62] X. Yang, R.A. Jones, M.J. Wiester, Dalton Trans. (2004) 1787.
[63] M. Albrecht, O. Osetska, R. Frohlich, Dalton Trans. (2005) 3757.
[64] R.D. Rogers, A.N. Rollins, R.F. Henry, J.S. Murdoch, R.D. Etzenhouser, S.E. Huggins, L. Nunez, Inorg. Chem. 30 (1991) 4946.
[65] J.-S. Li, B. Neumuller, K. Dehnicke, Z. Anorg. Allg. Chem. 628 (2002) 933.
[66] L. Yang, D. Xie, Y. Xu, Y. Wang, S. Zhang, S. Weng, K. Zhao, J. Wu, J. Inorg. Biochem. 99 (2005) 1090.
[67] L. Yang, Y. Xu, Y. Wang, S. Zhang, S. Weng, K. Zhao, J. Wu, Carbohydr. Res. 340 (2005) 2773.
[68] N. Brianese, U. Casellato, S. Tamburini, P. Tomasin, P.A. Vigato, Inorg. Chem. Commun. 2 (1999) 149.
[69] P. Sobato, J. Utko, K. Sztajnowska, L.B. Jerzkiewicz, New J. Chem. 22 (1998) 851.
[70] R.D. Rodgers, R.D. Etzenhouser, Acta Crystallogr., Sect. C 44 (1988) 1400.
[71] R.D. Rogers, R.D. Etzenhouser, Acta Crystallogr., Sect. C 44 (1988) 1533.
[72] B.C. Chakoumakos, R. Custelcean, J.O. Ramey, J.A. Kolopus, R. Jin, J.S. Neal, D.J. Wisniewska, L.A. Boatner, Cryst. Growth Des. 8 (2008) 2070.

[73] L.A. Boatner, D. Wisniewska, J.S. Neal, J.O. Ramey, J.A. Kolopus, B.C. Chakoumakos, M. Wisniewska, R. Custelcean, Appl. Phys. Lett. 93 (2008) 244104.
[74] D. Massiot, F. Fayon, M. Capron, I. King, S. Le Calve, B. Alonso, J.-O. Durand, B. Bujoli, Z. Gan, G. Hoatson, Mag. Res. Chem. 40 (2002) 70.
[75] M.A. Rodriguez, T.J. Boyle, P. Yang, D.L. Harris, Powder Diffract. 23 (2008) 121.
[76] T.J. Boyle, L.A.M. Ottley, M.A. Rodriguez, R.M. Sewell, T.M. Alam, S.K. McIntyre, Inorg. Chem. 47 (2008) 10708.
[77] K. Asakura, T. Imamoto, Bull. Chem. Soc. Jpn 74 (2001) 731.
[78] G.B. Deacon, T. Feng, P.C. Junk, G. Meyer, N.M. Scott, B.W. Skelton, A.H. White, Aust. J. Chem. 53 (2000) 853.
[79] M.J. Glazier, W. Levason, M.L. Matthews, P.L. Thornton, Inorg. Chim. Acta 357 (2004) 1083.
[80] A. Mandel, J. Magull, Z. Anorg. Allg. Chem. 623 (1997) 1542.
[81] S. Petricek, Polyhedron 22 (2004) 2293.
[82] S. Petricek, Z. Anorg. Allg. Chem. 631 (2005) 1947.
[83] C. Runschke, G. Meyer, Z. Anorg. Allg. Chem. 623 (1997) 981.
[84] N.J. Hill, W. Levason, M.C. Popham, G. Reid, M. Webster, Polyhedron 21 (2002) 1579.
[85] T. Heuer, F. Steffen, G. Meyer, Eur. J. Solid State Inorg. Chem. 33 (1996) 265.
[86] S. Ishikawa, T. Hamada, K. Manabe, S. Kobayashi, J. Am. Chem. Soc. 126 (2004) 12236.
[87] J. Fawcett, A.W.G. Platt, S. Vickers, M.D. Ward, Polyhedron 23 (2004) 2561.
[88] P.B. Hitchcock, A.G. Hulkes, M.F. Lappert, Inorg. Chem. 43 (2004) 1031.
[89] G.B. Deacon, T. Feng, S. Nickel, B.W. Skelton, A.H. White, Chem. Commun. 17 (1993) 1328.
[90] L.S. Smith, D.C. McCain, D.L. Wertz, J. Am. Chem. Soc. 98 (1976) 5125.
[91] J.-C. Berthet, M. Nierlich, M. Ephritikhine, Polyhedron 22 (2003) 3475.
[92] J.-C. Berthet, C. Riviere, Y. Miquel, M. Nierlich, C. Madic, M. Ephritikhine, Eur. J. Inorg. Chem. (2002) 1439.
[93] W.J. Evans, R.N.R. Broomhall-Dillard, J.W. Ziller, Polyhedron 17 (1998) 3361.
[94] L. Karmazin, M. Mazzanti, J.-P. Bexombes, C. Gateau, J. Pecaut, Inorg. Chem. 43 (2004) 5147.
[95] L. Karmazin, M. Mazzanti, C. Gateau, C. Hill, J. Pecaut, Chem. Commun. (2002) 2892.
[96] A. Sen, V. Chebolu, E.M. Holt, Inorg. Chim. Acta 118 (1986) 87.
[97] V. Chebolu, R.R. Whittle, A. Sen, Inorg. Chem. 24 (1985) 3082.
[98] K. Izod, S.T. Liddle, W. Clegg, Inorg. Chem. 43 (2004) 214.
[99] G.V. Khoroshen'kov, A.A. Fagin, M.N. Bochkarev, S. Dehert, Russ. Chem. Bull. 52 (2003) 1715.
[100] S.T. Liddle, P.L. Arnold, Organometallics 24 (2005) 2597.
[101] M. Niemeyer, Acta Crystllogr., Sect. E 57 (2001) M363.
[102] A.A. Trifonov, P. van de Weighe, J. Colin, A. Domingos, I. Santos, J. Organomet. Chem. 527 (1997) 225.
[103] S. Anfang, K. Dehnicke, J. Magull, Z. Naturforsch., B: Chem. Sci. 51 (1996) 531.
[104] R.B. Balashova, G.V. Khoroshen'kov, D.M. Kuzyaev, I.L. Eremmenko, G.G. Aleksandrov, G.K. Fukin, M.N. Bochkarev, Russ. Chem. Bull. (2004) 825.
[105] W.J. Evans, G.W. Rabe, J.W. Ziller, Inorg. Chem. 33 (1994) 3072.
[106] L. Huebner, A. Komienko, T.J. Emge, J.G. Brennan, Inorg. Chem. 43 (2004) 5659.
[107] R. Wietzke, M. Mazzanti, J.-M. Latour, J. Pecaut, J. Chem. Soc., Dalton Trans. (2000) 4167.
[108] Z. Xie, K. Chiu, B. Wu, T.C.W. Mak, Inorg. Chem. 35 (1996) 5957.
[109] F.-G. Yuan, Q. Shen, J. Sun, Chem. J. Chin. Univ. 22 (2001) 1501.
[110] C. Riviere, M. Nierlich, M. Ephritikhine, C. Madic, Inorg. Chem. 40 (2001) 4428.
[111] A. Cabrera, M. Slamon, N. Rosas, J. Perz-Flores, L. Velasco, G. Espinosa-Perez, J.L. Aria, Polyhedron 17 (1998) 193.
[112] M. Vestergren, B. Gustafsson, A. Johansson, M. Hakansson, J. Organomet. Chem. 689 (2004) 1723.
[113] T.V. Balashova, D.M. Kusayev, T.I. Kulikova, O.N. Kuznetsova, F.T. Edelmann, S. Giessmann, S. Blaurock, M.N. Bochkarev, Z. Anorg. Allg. Chem. 633 (2007) 256.
[114] L. Natrajan, J. Pecaut, M. Mazzanti, C. LeBrun, Inorg. Chem. 44 (2005) 4756.
[115] H. Mattausch, C. Hoch, A. Simon, Z. Anorg. Allg. 631 (2005) 1423.
[116] A. Babai, A.-V. Mudring, Inorg. Chem. 45 (2006) 4874.
[117] S. Anfang, M. Karl, N. Faza, W. Massa, J. Majull, Z. Anorg. Allg. Chem. 623 (1997) 1425.
[118] M. Mazzanti, R. Wietzke, J. Pecaut, J.-M. Latour, P. Maidivi, M. Remy, Inorg. Chem. 41 (2002) 2389.
[119] K.J. Ooms, K.W. Feindel, M.J. Willans, R.E. Wasylishen, J.V. Hanna, K.J. Pike, M.E. Smith, Solid State NMR 28 (2005) 125.
[120] B.M. Herreros, P.P. Man, J.M. Manoli, J. Fraissard, J. Chem. Soc., Chem. Commun. (1992) 464.
[121] M.J. Willians, K.W. Feindel, K.J. Ooms, R.E. Wasylishen, Chem.-A Eur. J. 12 (2005) 159.
[122] M. Hunger, G. Engelhardt, J. Weitkamp, Microporous Mater. 3 (1995) 497.